Skeletal Radiology (2019) 48:1891–1898
https://doi.org/10.1007/s00256-019-03221-0

SCIENTIFIC ARTICLE

Radiographic signs of hook of hamate fracture: evaluation of diagnostic utility

Jayden Spencer[1] · Suzanne L. Hunt[2] · Chuanwu Zhang[2] · Carissa Walter[1] · Brian Everist[1]

Received: 21 January 2019 / Revised: 8 April 2019 / Accepted: 9 April 2019 / Published online: 27 May 2019

Abstract

Objective Hook of hamate fracture, the most common swing-related wrist fracture, is commonly seen in high-level athletes. The fracture is rarely diagnosed on routine wrist radiographs, thus generally requiring CT or MR for diagnosis. Surgical excision has a high success rate, however diagnostic delay contributes to a high complication rate. Radiographic signs of hook of hamate fracture have been published, but uncertainty of the diagnostic accuracy limits application. The purpose of this study is to determine accuracy and interobserver reliability of radiographic signs of hook of hamate.

Materials and methods This retrospective case-control study evaluated wrist radiographs of 50 patients, including 24 positive and 26 negative, for hook of hamate fracture, each proven by CT or MR. Five reviewers performed blinded, randomized evaluation of radiographs documenting whether the hook of hamate was normal or fractured, and if fractured, the radiographic signs present (ring sign, ghostly shadow, and diffuse sclerosis) and views that contributed to diagnosis.

Results Radiographic signs demonstrated high sensitivity (85%; 95% CI: 77–91), specificity (92%; 95% CI: 86–96), and accuracy (89%; 95% CI: 84–92) with substantial interobserver reliability (k = 0.652). The ring sign was the most sensitive radiographic sign. Diagnosis was most often supported by the oblique view (38%) and rarely the lateral view (15%).

Conclusions Radiographic signs of hook of hamate fracture on routine radiographs can accurately and reliably diagnose hook of hamate fractures. Evaluation for discontinuity of the cortical ring will optimize sensitivity, allowing for timely diagnosis and treatment, and a reduction of complications.

Keywords Hook of hamate · Fracture · Radiograph · Radiographic signs

Introduction

The hamate is located on the ulnar side of the wrist in the distal carpal row. The hook of hamate is a curved, hook-like process that projects 1–2 cm distally and radially from the palmar aspect of the hamate (Fig. 1). It forms the ulnar border of the carpal tunnel and the radial border of Guyon's canal. Multiple ligaments and tendons attach to the hook of hamate and its lateral surface is grooved for passage of the flexor tendons [1, 2].

Fractures of the hamate account for approximately 2% of carpal fractures [3, 4]. However, fracture of the hook of hamate, the most commonly reported swing-related wrist fracture, has gained attention in sports medicine due to prevalence in high-level athletes in golf and baseball [5–9]. The butt of the club or bat abuts the non-dominant hand over the hook of hamate and fracture occurs via leverage mechanism. It is reported to be more common in professional than amateur athletes, due to the high force and repetitive stress required to

✉ Jayden Spencer
jspencer2@kumc.edu

Suzanne L. Hunt
shunt@kumc.edu

Chuanwu Zhang
czhang4@kumc.edu

Carissa Walter
cwalter2@kumc.edu

Brian Everist
beverist@kumc.edu

[1] Department of Radiology, Kansas University Hospital, 3901 Rainbow Blvd, MS 4032, Kansas City, KS 66160, USA

[2] Department of Biostatistics, Kansas University Hospital, 3901 Rainbow Blvd, MS 1026, Kansas City, KS 66160, USA

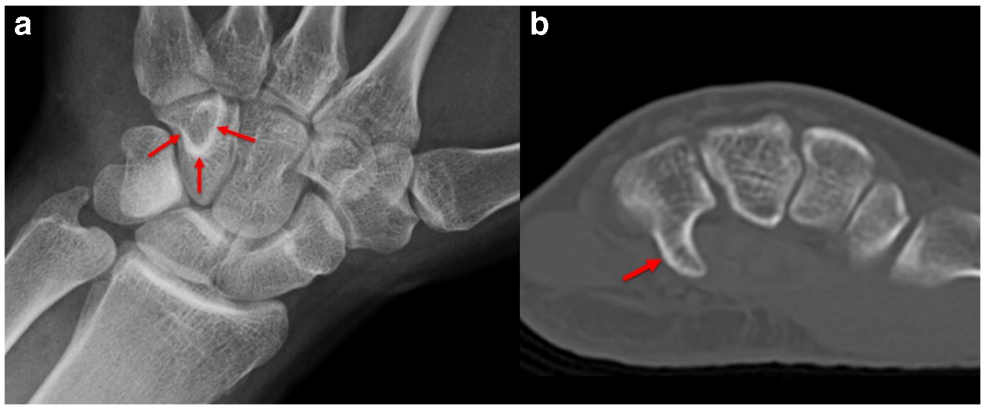

Fig. 1 Posteroanterior (PA) radiograph (**a**) of the left wrist in a 35-year-old male demonstrating the normal appearance of the hook of hamate. The basal cortical ring (*arrows*), corresponding to the base of the hook of hamate is seen en face. Axial CT (**b**) shows normal appearance of the hook of hamate (*arrow*)

cause fracture [5, 8–10]. Retrospective studies have demonstrated nonunion rates ranging from 50 to 90% with very few cases of healing by immobilization reported [6, 11–13]. Diagnostic delay, poor vascularity, and frequent motion contribute to the high rate of nonunion [12, 13]. Athletes often report gradual onset of pain rather than a single traumatic event and often continue to practice, which can result in significant complications including damage to the adjacent flexor tendons, artery, or nerve, and secondary osteoarthritis [6, 8, 12–17]. The current standard of treatment in athletes is surgical excision, which has a high success rate and relatively short recovery time, with athletes usually returning to full activity in 4–8 weeks [18–23].

Fracture of the hook of the hamate is rarely diagnosed on routine three-view wrist radiographs, the standard initial diagnostic imaging study. Carpal tunnel and semisupine oblique views have higher diagnostic accuracy, but are not acquired unless there is suspicion for hook of hamate fracture [24–26]. Ultimately, computed tomography (CT) or magnetic resonance (MR) imaging is necessary to confirm the diagnosis and extent of injury. Radiographic signs of hook of hamate fracture have been published, but uncertainty of the diagnostic accuracy limits large scale application [24–27]. The purpose of this project was to determine the sensitivity, specificity, accuracy, and interobserver reliability of radiographic signs of the hook of hamate fracture and which of the routine projections demonstrate the fracture, to enable more accurate and timely diagnosis.

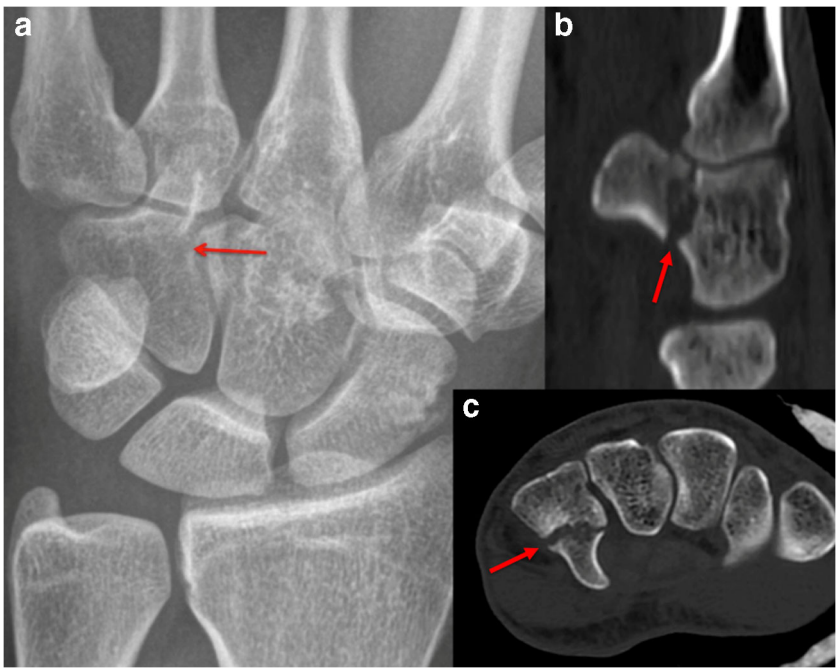

Fig. 2 A 23-year-old male 2 weeks following left wrist injury in a motorcycle accident. PA radiograph (**a**) demonstrates discontinuity of the basal cortical ring of the hook of hamate, "ring sign" (*arrow*). A scaphoid waist fracture is also noted. Sagittal (**b**) and axial CT (**c**) images performed the following day confirm a minimally displaced fracture at the base of the hook of hamate with mild osseous resorption at the fracture margins

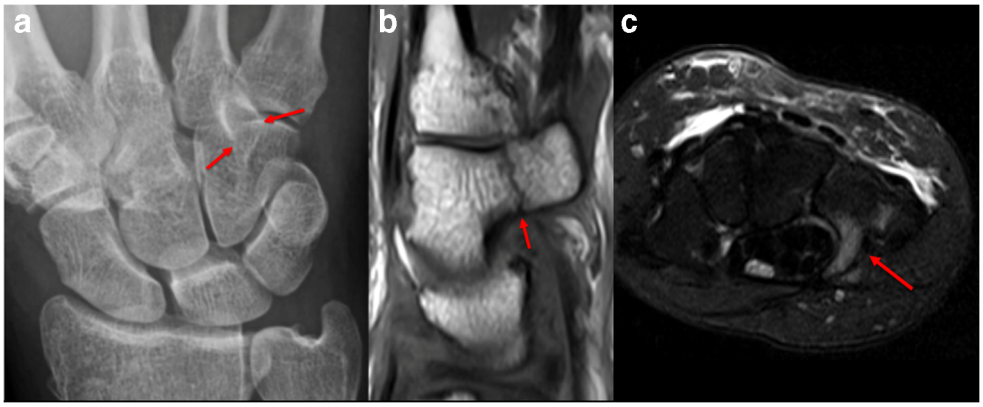

Fig. 3 A 48-year-old male with right wrist pain after falling off a bicycle on an outstretched hand earlier the same day. PA radiograph (**a**) demonstrates discontinuity of the cortical ring of the hook of hamate, "ring sign" (*arrows*). Sagittal T1 (**b**) and axial T2 fat-saturated (**c**) MR images performed 11 days following the radiograph confirm a nondisplaced fracture of the hook of hamate with surrounding marrow edema (*arrows*)

Methods

Data collection

Following institutional review board approval, a retrospective review of a single institution's radiology database was queried for CT and MR imaging reports with the keywords "hook of hamate" and "fracture". Control patients were randomly selected from the radiology database queried for reports with indications of "evaluate for fracture", "injury", or "trauma" in which no fracture was identified. Results of CT or MR imaging were considered the "gold standard" for defining whether a fracture of the hook of hamate was present. Subjects were collected from imaging studies performed from January 1, 2000 to July 31, 2016. Patients were excluded from the study if a routine wrist radiograph series was not available within 1 month prior to cross-sectional imaging. Additional data collected included demographics and when available, mechanism of injury, clinical diagnostic and treatment information, and outcome of treatment.

Imaging evaluation

Five fellowship-trained musculoskeletal radiologists independently interpreted images following brief review of nomenclature and examples of the three published radiographic signs of hook of hamate fracture, all of which are based on the PA view. The radiographic signs included: (1) "Ring sign", which refers to discontinuity of the hook of hamate cortical ring [25] (Figs. 2 and 3), (2) "Ghostly shadow", which refers to nonvisualization of the hook of hamate with lucency in its expected location, reflecting a displaced fracture (Fig. 4) [22], and (3) "Diffuse sclerosis" of the hook of hamate with poor delineation of the cortical ring, reflecting sclerosis of the fracture margins in cases of nonunion (Fig. 5) [22]. The five musculoskeletal radiologists, blinded to the diagnosis from MR or CT, reviewed routine three-view wrist radiographs of all 50 patients. The reviewers documented whether each case was positive or negative for hook of hamate fracture and which, if any, radiographic sign(s) were identified. The radiograph interpretation was negative if no radiographic signs were identified; whereas, if any one of the radiographic signs was identified, the interpretation was considered positive for fracture. For the radiographs diagnosed with fractures, the radiologists documented the projection(s) in which the fracture was identified. Utilizing the MR or CT diagnosis as the standard of reference, the data were analyzed to determine the sensitivity, specificity, and accuracy of the radiographic signs, as well as the interobserver reliability.

Statistical analysis

Descriptive statistics (sensitivity, specificity, accuracy) are reported for each radiographic sign individually and when used in combi-

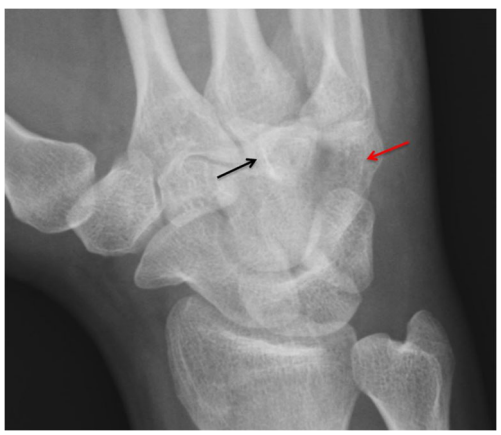

Fig. 4 Oblique radiograph (*left*) demonstrates lucency projecting over the hamate in the expected location of the hook of hamate, i.e., "Ghostly shadow" (*red arrow*). Radial and distal displacement of the fracture fragment (*black arrow*) is also seen, confirmed on MRI performed 1 week later

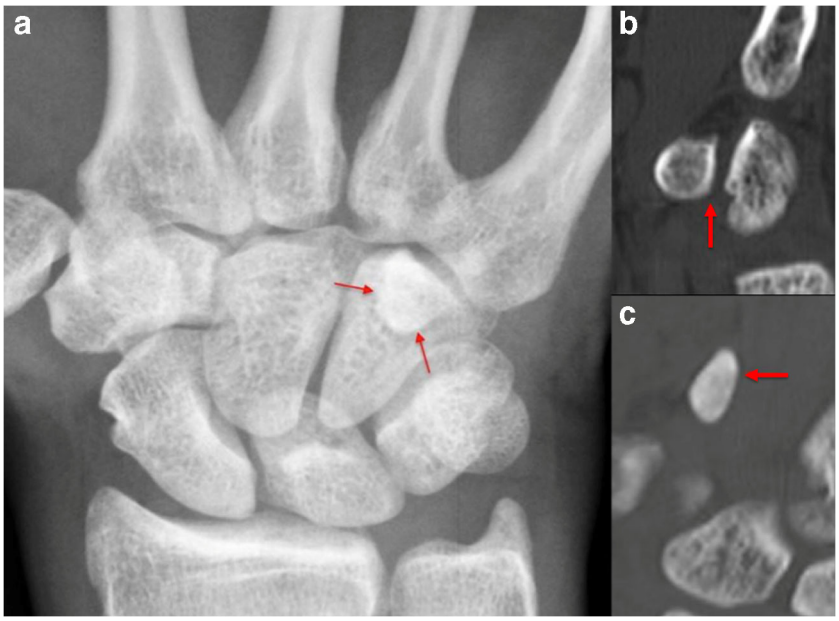

Fig. 5 A 32-year-old avid golfer referred for persistent ulnar sided wrist pain for 1 year, exacerbated by swinging a golf club. PA radiograph (**a**) demonstrates diffusely sclerotic appearance of the hook of hamate. Sagittal (**b**) and coronal CT (**c**) demonstrate sclerosis of the fracture margins, consistent with nonunion. Coronal image **c** is through the neocortex cross referencing to the level of the *arrow* in image **b**

Table 1 Baseline characteristics of the cohort

Measure	All	Fracture	No fracture	*p* value[a]
N	50	24	26	
Age at X-ray, median (IQR)	46.0 (31.8, 54.5)	31.9 (22.4, 44.5)	51.9 (49.1, 57.5)	< 0.001
Male, *n* (%)	27 (54.0%)	15 (62.5%)	12 (46.2%)	0.25
Ethnicity, *n* (%)				0.55
Non-Hispanic/Latino, *n* (%)	44 (88.0%)	21 (87.5%)	23 (88.5%)	
Hispanic/Latino, *n* (%)	5 (10.0%)	2 (8.3%)	3 (11.5%)	
Unknown ethnicity, *n* (%)	1 (2.0%)	1 (4.2%)	0 (0.0%)	
Race, *n* (%)				0.71
Black, *n* (%)	9 (18.0%)	3 (12.5%)	6 (23.1%)	
White, *n* (%)	36 (72.0%)	19 (79.2%)	17 (65.4%)	
Other race, *n* (%)	3 (6.0%)	1 (4.2%)	2 (7.7%)	
Unknown race, *n* (%)	2 (4.0%)	1 (4.2%)	1 (3.8%)	
Side injured, *n* (%)				0.82
Right, *n* (%)	20 (40.0%)	10 (41.7%)	10 (38.5%)	
Left, *n* (%)	30 (60.0%)	14 (58.3%)	16 (61.5%)	
Cause of injury, *n* (%)				
Fall, *n* (%)	8 (16.0%)	4 (16.7%)	4 (15.4%)	
Motor vehicle accident, *n* (%)	5 (10.0%)	5 (20.8%)	0 (0.0%)	
Swinging sports, *n* (%)	8 (16.0%)	6 (25.0%)	2 (7.7%)	
Punch, *n* (%)	4 (8.0%)	3 (12.5%)	1 (3.8%)	
Other/unknown, *n* (%)	25 (50.0%)	6 (25.0%)	19 (73.1%)	
Pre-treatment complication, *n* (%)				
ECU tendon tear, *n* (%)	5 (10.0%)	4 (16.7%)	1 (3.8%)	
ECU tenosynovitis, *n* (%)	3 (6.0%)	2 (8.3%)	1 (3.8%)	
Ulnar neuropathy, *n* (%)	1 (4.2%)	1 (4.2%)	0 (0.0%)	
Imaging modality, *n* (%)				< 0.001
CT, *n* (%)	15 (30.0%)	11 (45.8%)	4 (15.4%)	
MR, *n* (%)	30 (60.0%)	8 (33.3%)	22 (84.6%)	
Both, *n* (%)	5 (10.0%)	5 (20.8%)	0 (0.0%)	

[a] *p* values calculated by Kruskal–Wallis test for continuous variables, Chi-square test for categorical variables, and Fisher's exact test for categorical variables with low expected cell counts

Table 2 Radiographic interpretation: overall and radiographic signs independently

Overall		
Interpretation	Fracture ($N = 120$)	No fracture ($N = 130$)
Positive	102	10
Negative	18	120
By radiographic sign		
Ring sign		
Yes	69	9
No	51	121
Ghostly shadow		
Yes	20	1
No	100	129
Diffuse sclerosis		
Yes	24	0
No	96	130

nation for the diagnosis of hook of hamate fractures. Accuracy was calculated as the sum of the true positives and true negatives, divided by the total number of cases. The 95% confidence intervals are reported and κ coefficient is calculated to determine interobserver reliability. Statistical significance is defined as P value < 0.05. All data management and statistical analysis is done in SAS 9.4.

Results

Demographics

From the radiology database search, 24 patients met the inclusion criteria for the case group, i.e., positive for hook of hamate fracture on CT or MR with wrist radiographs obtained prior to cross-sectional imaging. Of the 24 hook of hamate fractures, 16 were diagnosed as acute or subacute and eight were diagnosed as chronic or nonunion on cross-sectional imaging. Twenty-six patients from the radiology database search with CT or MR negative for hook of hamate fracture were randomly selected for the control group. Table 1 displays patients' demographics with no statistically significant differences between the two groups apart from patient age.

Imaging interpretation

Fifty wrist radiographs were independently evaluated by five radiologists resulting in a total of 250 blinded interpretations. The results from blinded interpretations are listed in Table 2. A total of 112 of the 250 radiographic evaluations were interpreted as positive for hook of hamate fracture, comprising 102 true positives and ten false positives. In total, 112 positive interpretations, a radiographic sign of hook of hamate fracture was reported on the PA view. The next most commonly reported projection demonstrating the fracture was the oblique view (Figs. 4 and 6b), followed by the lateral view (Fig. 7b), reported in 42 (38%) and 17 (15%) of the positive interpretations, respectively.

Table 3 summarizes the observed sensitivity, specificity, and accuracy of the radiographic signs overall and individually. Overall diagnostic interpretation, utilizing any of the three radiographic signs, resulted in sensitivity of 85%, specificity of 92.3%, and accuracy of 88.9%. The "ring sign", "ghostly shadow", and diffuse sclerosis were observed in 78, 21, and 24 of the interpretations, respectively. The "ring sign" had a sensitivity of 57.5%, specificity of 93.1%, and accuracy of 76%. The "ghostly shadow" had a sensitivity of 16.7%, specificity of 99.2%, and accuracy of 59.6%. Diffuse sclerosis had a sensitivity of 20%, specificity of 100%, and accuracy of 61.6%. In 101 of the 112 positive interpretations, a single radiographic sign was present and in 11 of the 112, two signs were present.

The results from blinded interpretations for the individual readers are listed in Table 4 and the observed sensitivity, specificity, and accuracy of the radiographic signs for the individual readers are listed in Table 5. κ coefficient values were

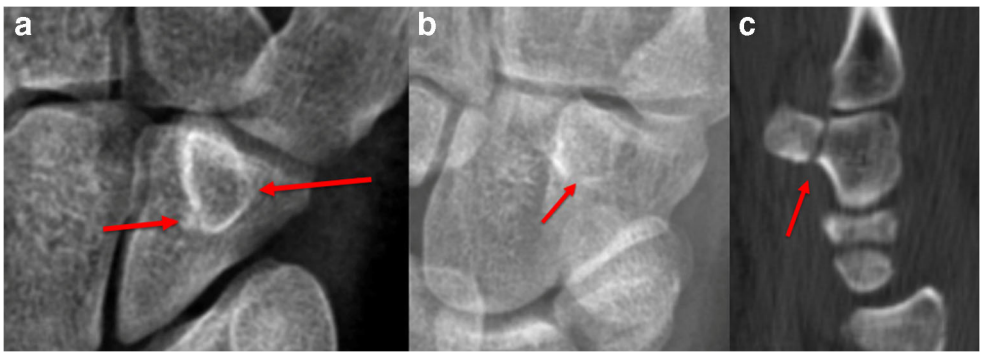

Fig. 6 A 31-year-old male with right wrist pain following motorcycle accident. PA (**a**) and oblique radiographs (**b**) demonstrate subtle discontinuity of the basal cortical ring of the hook of hamate, i.e., "ring sign" (*arrows*). Sagittal CT (**c**) performed the same day confirms a mildly displaced fracture at the base of the hook of hamate (*arrow*)

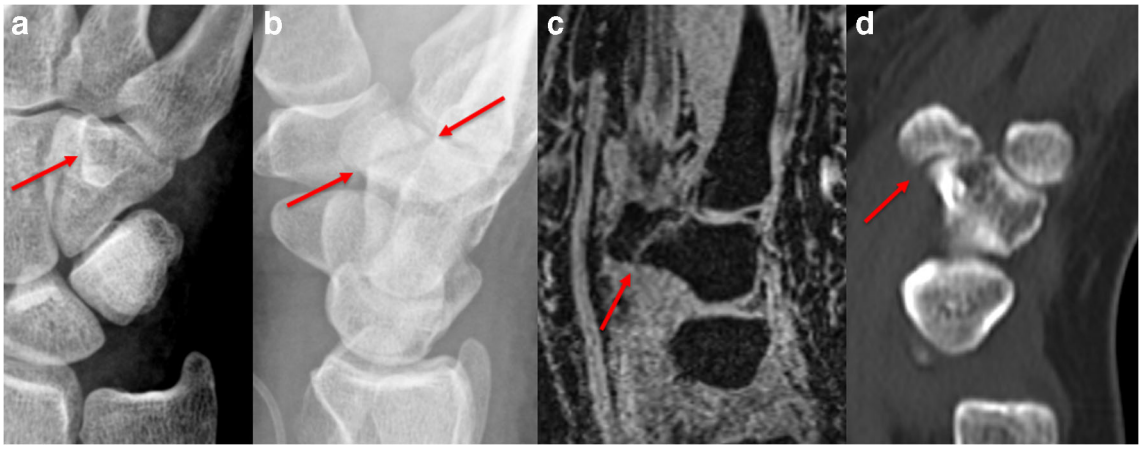

Fig. 7 A 29-year-old female with right wrist pain following motor vehicle collision. PA radiograph (**a**) demonstrates discontinuity of the hook of hamate cortical ring and lateral radiograph (**b**) demonstrates oblique linear lucency through the hook of hamate. Sagittal T1 volumetric interpolated breath-hold exam (VIBE) 3D MR image (**c**) performed 13 days following the radiographs confirms the diagnosis of a nondisplaced oblique fracture through the hook of hamate and T2 images (not shown) demonstrated marrow edema surrounding the fracture. Sagittal CT image (**d**) following 2 months of conservative management demonstrates mild displacement of the fracture with partially sclerotic fracture margins and no evidence of healing

calculated on the initial blinded review by the individual readers. The observed κ coefficient of 0.652 reflects substantial interobserver agreement among the five radiologists utilizing radiographic signs for diagnosis of hook of hamate fracture.

Discussion

In this study, the "ring sign" was the most sensitive radiographic sign, which was expected, since any type of hook of hamate fracture may show discontinuity of the cortical ring. Diffuse sclerosis reflects sclerotic fracture margins and therefore its utility is limited to chronic fractures and suggests nonunion. Absence of the hook or the "ghostly shadow" was the least sensitive of the radiographic signs, although was highly specific at 99.2%, reflecting its limited utility to significantly displaced fractures. Diffuse sclerosis was reported in 26 of the 40 evaluations of cases diagnosed as chronic on cross-sectional imaging, corresponding to a sensitivity of 65%, when specifically applied to chronic hook of hamate fractures. Finally, diffuse sclerosis or any two of the three radiographic signs was 100% specific for hook of hamate fracture, comprising 24 and 11 of the true-positive interpretations, respectively.

Table 3 Observed diagnostic utility of radiographic signs: overall and independently

Overall			
	Sensitivity (%)	Specificity (%)	Accuracy (%)
Observed	85.0	92.3	88.9
95% CI	77.3–90.9	86.3–96.3	84.2–92.4
By radiographic sign			
Ring sign	57.5	93.1	76.0
Ghostly shadow	16.7	99.2	59.6
Diffuse sclerosis	20.0	100	61.6

Close inspection of the cortical ring of the hook of hamate on the PA view for discontinuity, i.e., "ring sign", will optimize the sensitivity of screening radiographs. The "ghostly shadow" and diffuse sclerosis have lower sensitivity, although when present, allow more confident diagnosis of hook of hamate fractures. When a radiographic sign of hook of hamate fracture is identified on the PA view, the diagnosis can sometimes be confirmed on the oblique view and rarely on the lateral view. Diagnosis can often be achieved with carpal tunnel or semisupine oblique radiographs. CT and MR allow definitive diagnosis and evaluation for complications. Stress fractures, common in swinging athletes, often require MR for diagnosis. When there is a lower degree of suspicion, correlation for point tenderness over the hypothenar eminence is a reasonable next step prior to obtaining additional diagnostic imaging.

Potential limitations of the study include the fact that the interpreting radiologists were specifically instructed to evaluate for radiographic signs of hook of hamate fracture with knowledge that a fracture was present in a certain,

Table 4 Individual reader radiograph interpretations: readers A, B, C, D, and E

Interpretation	Reader A overall		Reader B overall		Reader C overall		Reader D overall		Reader E overall	
	Fracture (*N* = 24)	No fracture (*N* = 26)	Fracture (*N* = 24)	No fracture (*N* = 26)	Fracture (*N* = 24)	No fracture (*N* = 26)	Fracture (*N* = 24)	No fracture (*N* = 26)	Fracture (*N* = 24)	No fracture (*N* = 26)
Positive	20	3	21	0	18	2	20	5	23	0
Negative	4	23	3	26	6	24	4	21	1	26
	Reader A By radiographic sign		Reader B By radiographic sign		Reader C By radiographic sign		Reader D By radiographic sign		Reader E By radiographic sign	
Ring sign										
Yes	13	3	15	0	8	2	16	4	17	0
No	11	23	9	26	16	24	8	22	7	26
Ghostly shadow										
Yes	2	0	5	0	7	0	3	1	3	0
No	22	26	19	26	17	26	21	25	21	26
Diffuse sclerosis										
Yes	7	0	6	0	4	0	3	0	4	0
No	17	26	18	26	20	26	21	26	20	26

although unknown, percentage of cases. Small sample size is an additional limitation of the study. Potential pitfalls of the radiographic signs of hook of hamate fracture include stress fractures or other radiographically occult fractures, hypoplasia or aplasia, an unfused ossification center, previous resection, ganglion cysts, and various arthropathies resulting in erosive or cystic changes of the hook of hamate [24, 28, 29]. Rarely, an osteoid osteoma of the hamate can result in diffuse sclerosis of the hook of hamate, mimicking a nonunited fracture [30]. Future studies could confirm the diagnostic performance of the radiographic signs with greater power by evaluating a larger number of cases. Pain associated with hook of hamate fractures is often less than typically associated with fractures and for this reason, many patients do not initially seek treatment or do not proceed with cross-sectional imaging when initial radiographs are negative. Overall prevalence of hook of hamate fractures, especially nondisplaced stress fractures, likely remains underestimated and future studies could further investigate prevalence and the value of earlier detection.

Conclusions

This study demonstrates that by implementing radiographic signs of hook of hamate fractures, routine view wrist radiographs can achieve adequate sensitivity, specificity, and accuracy in the diagnosis of hook of hamate fractures with substantial interobserver reliability. Application of these radiographic signs can help to avoid diagnostic delay and associated complications.

Table 5 Individual reader observed diagnostic utility: readers A, B, C, D, and E

	Reader A overall			Reader B overall			Reader C overall			Reader D overall			Reader E overall		
	Sens (%)	Spec (%)	Acc (%)	Sens (%)	Spec (%)	Acc (%)	Sens (%)	Spec (%)	Acc (%)	Sens (%)	Spec (%)	Acc (%)	Sens (%)	Spec (%)	Acc (%)
Observed	83	89	86	88	100	94	75	92	84	83	81	82	96	100	98
95% CI	63–95	70–98	73–94	68–97	87–100	83–99	53–90	75–99	71–93	63–95	61–94	69–91	79–100	87–100	89–100
	Reader A By radiographic sign			Reader B By radiographic sign			Reader C By radiographic sign			Reader D By radiographic sign			Reader E By radiographic sign		
Ring sign	54	89	72	63	100	82	33	92	64	67	85	76	71	100	86
Ghostly shadow	8	100	56	21	100	62	29	100	66	13	96	56	13	100	58
Diffuse sclerosis	29	100	66	25	100	64	17	100	60	13	100	58	17	100	60

Acknowledgements Thanks to Brian Everist, MD, Douglas Nelson, MD, Gary Hinson, MD, Kevin Brown, MD, and Anders Grinde, MD for contributing their time and expertise to imaging interpretations. Thanks to Lauren Clark, MS and Shelby Bell for their contributions to statistical analysis.

Compliance with ethical standards

Conflict of interest The authors declare that they have no conflicts of interest.

References

1. Mesgarzadeh M, Schneck CD, Bonakdarpour A. Carpal tunnel: MR imaging. Part I. Normal anatomy. Radiology. 1989;171(3):743–8.
2. Eathorne SW. The wrist: clinical anatomy and physical examination—an update. Primary Care. 2005;32(1):17–33.
3. Urch EY, Lee SK. Carpal fractures other than scaphoid. Clin Sports Med. 2015;34(1):51–67.
4. Suh N, Ek ET, Wolfe SW. Carpal fractures. J Hand Surg Am. 2014;39(4):785–91.
5. Helms CA. Fundamentals of skeletal radiology. Elsevier Health Sciences; 2013.
6. Bishop AT, Beckenbaugh RD. Fracture of the hamate hook. J Hand Surg. 1988;13.1:135–9.
7. Stark HH, Jobe FW, Boyes JH, Ashworth CR. Fracture of the hook of the hamate in athletes. J Bone Joint Surg Am. 1977;59(5):575–82.
8. Aldridge JM, Mallon WJ. Hook of the hamate fractures in competitive golfers: results of treatment by excision of the fractured hook of the hamate. Orthopedics. 2003;26(7):717–9.
9. Murray PM, Cooney WP. Golf-induced injuries of the wrist. Clin Sports Med. 1996;15(1):85–109.
10. Parker RD, Berkowitz MS, Brahms MA, Bohl WR. Hook of the hamate fractures in athletes. Am J Sports Med. 1986;14(6):517–23.
11. Roach JJ. Compound incomplete dislocation of the trapezium and compound fractured hamate hook. J Natl Med Assoc. 1978;70(11):841.
12. Foucher G, Schuind F, Merle M, Brunelli F. Fractures of the hook of the hamate. J Hand Surg. 1985;10(2):205–10.
13. David TS, Zemel NP, Mathews PV. Symptomatic, partial union of the hook of the hamate fracture in athletes. Am J Sports Med. 2003;31(1):106–11.
14. Kaplan EB. Functional & Surgical anatomy of the hand. JP Lippincott; 1965.
15. Boulas HJ, Milek MA. Hook of the hamate fractures. Diagnosis, treatment, and complications. Orthopaed Rev. 1990;19(6):518–29.
16. Murray WT, Meuller PR, Rosenthal DI, Jauernek RR. Fracture of the hook of the hamate. Am J Roentgenol. 1979;133(5):899–903.
17. Futami T, Aoki H, Tsukamoto Y. Fractures of the hook of the hamate in athletes: 8 cases followed for 6 years. Acta Orthop Scand. 1993;64(4):469–71.
18. Stark HH, Chao EK, Zemel NP, Rickard TA, Ashworth CR. Fracture of the hook of the hamate. J Bone Joint Surg Am. 1989;71(8):1202–7.
19. Bachoura A, Wroblewski A, Jacoby SM, Osterman AL, Culp RW. Hook of hamate fractures in competitive baseball players. Hand. 2013;8(3):302–7.
20. Devers BN, Douglas KC, Naik RD, Lee DH, Watson JT, Weikert DR. Outcomes of hook of hamate fracture excision in high-level amateur athletes. J Hand Surg. 2013;38(1):72–6.
21. Smith P, Wright TW, Wallace PF, Dell PC. Excision of the hook of the hamate: a retrospective survey and review of the literature. J Hand Surg. 1988;13(4):612–5.
22. Scheufler O, Andresen R, Radmer S, Erdmann D, Exner K, Germann G. Hook of hamate fractures: critical evaluation of different therapeutic procedures. Plast Reconstr Surg. 2005;115(2):488–97.
23. O'Shea K, Weiland AJ. Fractures of the hamate and pisiform bones. Hand Clin. 2012;28(3):287–300.
24. Norman AL, Nelson JO, Green ST. Fractures of the hook of hamate: radiographic signs. Radiology. 1985;154(1):49–53.
25. Papilion JD, DuPuy TE, Aulicino PL, Bergfield TG, Gwathmey FW. Radiographic evaluation of the hook of the hamate: a new technique. J Hand Surg. 1988;13(3):437–9.
26. Kato H, Nakamura R, Horii E, Nakao E, Yajima H. Diagnostic imaging for fracture of the hook of the hamate. Hand Surg. 2000;5(01):19–24.
27. Andresen R, Radmer S, Sparmann M, Bogusch G, Banzer D. Imaging of hamate bone fractures in conventional X-rays and high-resolution computed tomography: an in vitro study. Investig Radiol. 1999;34(1):46–50.
28. Masada K, Kanazawa M, Fuji T. Flexor tendon ruptures caused by an intraosseous ganglion of the hook of the hamate. J Hand Surg. 1997;22(3):383–5.
29. Foster EJ, Palmer AK, Levinsohn EM. Hamate erosion: an unusual result of ulnar artery constriction. J Hand Surg. 1979;4(6):536–9.
30. Jackson WJ, Markiewitz AD. Osteoid osteoma of the hamate. Orthopedics. 2008;31(5).